Journal of the European Ceramic Society **19** (1999) 675–681
© 1999 Elsevier Science Limited
Printed in Great Britain. All rights reserved
PII: S0955-2219(98)00295-7 0955-2219/99/$ - see front matter

Mass and Charge Transport Involving Interfaces

Joachim Maier*

Max-Planck-Institut fair Festkörperforschung, Stuttgart, Germany

Abstract

The importance of interfaces for preparation, stability and performance of electroceramics is highlighted. Homo- (grain boundaries) and heterojunctions (internal phase boundaries, surfaces) are discussed in terms of their thermodynamic and kinetic influence on transport and reactivity. Special consideration is devoted to the treatment of space charge effects in the core-space-charge-model and the superposition of different pathways. © 1999 Elsevier Science Limited. All rights reserved

Keywords: interfaces, diffusion, electrical conductivity, space charges.

1 Introduction

Mass and charge transport, or in other words chemical and electrical transport are key processes for electroceramics for different reasons. The primary reason is the direct significance for the electroceramic function: resistors, capacitors, batteries, electrochemical sensors immediately rely on electrochemical processes (electroceramic performance). The secondary reason lies in the importance for preparation, annealing, conditioning, drift effects and degradation (pretreatment and stability of electroceramics). Interfacial effects can be detrimental, but also desired and even necessary, e.g. if the function makes direct use of interfacial processes (examples: ZnO-varistor, PTC-effect in $BaTiO_3$, Taguchi-sensors).

A bulk conductivity sensor may serve as a prototype example in this context. At higher temperatures $SrTiO_3$ reacts to slight changes of the ambient oxygen partial pressure by exhibiting significant changes in the bulk electrical conductivity. The signal to be detected is the electronic conductivity in the bulk. Electrode and grain boundary resistances are disadvantageous in this respect, including the possibility of short-circuits by highly conducting grain boundaries or surfaces.

The response time is determined by the rate and amount of oxygen dissolution. Requirements for a fast process are a high chemical diffusion coefficient D^{δ}, i.e. a high ambipolar conductivity (electronic and ionic conductivity, σ_{eon} and σ_{ion},) and a low chemical capacity (high thermodynamic factor, i.e. low defect densities). Also the effective surface rate constant for oxygen incorporation ($\bar{k}^{\delta}$) should be high while grain boundaries should not be blocking for mass transport. Highly permeable grain boundaries help to enhance the response time. D^{δ} and $\bar{k}^{\delta}$ should be low for other active species to depress cross-sensitivity as much as possible. Similar parameters (here the rôle of the less mobile ionic species (e.g. cations in anion conductors) is not at all negligible) determine the rate of preparation, including the rate of sintering. Similar parameters are decisive for degradation or poisoning processes (e.g. reaction of $SiTiO_3$ in exhaust atmospheres, dissolution of undesired impurities, etc.).

The sensor example not only highlights the double role of electrochemical transport but also the significance of the boundary processes. It is rather astonishing that not more work is devoted to the problem of interfacial transport properties of electroceramics. At least two reasons are responsible for this:

- the experimental difficulty of studying these phenomena, and not independent of that,
- the conceptional difficulties involved.

Boundary effects on transport phenomena are manifold; interfaces can act as transport pathways or transport barriers by virtue of the changed core structure (core effects) and by affecting the charge carrier distribution in the immediate neighbourhood (space charge effect). Moreover, in some cases the structural perturbation of a larger range is also essential (elastic and plastic deformation of the neighbourhood) (see e.g. Ref. 1).

Owing to the anisotropy of the boundaries, one has to distinguish between transport across and along interfaces. Both may come into play in the same material under the same conditions.[2]

---

*Fax: +49 711 689 1722; e-mail: weiglein@chemix.mpi-stuttgart.mpg.de

In addition, both electronic and ionic transport properties are often of simultaneous interest. All these properties do decisively depend on control parameters such as temperature, pressure, component potential, impurity content, not to mention kinetic constraints and time dependencies.

Moreover, size effects become increasingly prominent and their relevance for electroceramics needs to be clarified.

It will be shown that in spite of these difficulties, the defect chemistry of interfaces offers the basis of a systematic treatment. Since we are interested in the ionic and electronic properties and since their properties are far-reachingly analogous (ic), we always have a *mixed conductor* in mind.

The simplified treatment of boundary effects will be mainly based on the *abrupt core-space charge model* described.[3,4] For the consideration of mass transport the concepts of *chemical resistance* and *chemical capacitances* prove helpful.[5,6] The superposition of local properties to the overall property is achieved within the *generalised brick-layer model* described in Ref. 2.

Recent finite element calculations tested its validity and flexibility for resistive boundaries in many respects.[7]

2 Electrical Transport Across and Along Interfaces

2.1 Carrier redistribution at a single interface: core-space charge model

Internal interfaces are, in almost all cases, non-equilibrium defects. In other words, one cannot conclude from state variables (in particular: chemical composition) on the nature of the boundaries. At best, they are in local equilibrium, i.e. given T, p and chemical ambience but also topological and geometrical constraints, the boundary structure of lowest energy is well-defined.[8] In reality, however, even the realisation of this situation is not guaranteed and we may generally consider boundaries as irreversibly introduced two-dimensional structure elements. Thus structure and chemistry of a given boundary are to be determined experimentally. This core structure can offer particular carrier transport properties itself. Of high significance is the carrier redistribution occurring in the vicinity as a consequence of the structural singularity. In the simplest case we consider the chemical (ground) structure to vary in a step function way. At not too low temperatures, at least during preparation, ions or electrons can segregate or be injected.[9] In a homophase grain boundary this occurs symmetrically from or into the grain phase. At a hetero-phase contact, the behaviour is asymmetrical, and even a carrier redistribution affecting the boundary regions without excess charge in the core region is possible. The 'chemical' effect is counterbalanced by the electrical effect (i.e. $\Delta\tilde{\mu}_k = 0 = \Delta\mu_k + z_k F\phi$). The electric field not only restricts the redistribution in amount but also in extent (space charge regions), in that the boundary regions will (in partial equilibrium) be characterised by the usually small Debye-length (λ). A detailed consideration of the severe effects on the defect concentration is given elsewhere.[3,9] Here for simplicity we assume two singly charged carriers 1 and 2 to be important. There are essentially two cases to be distinguished. One is the realisation of a Gouy–Chapman type of profile,[10] which becomes hyperbolic for large effects. It occurs if all defects, or at least the majority carrier in the boundary regions can follow the electrical field. The concentration enhancement over the bulk values ($\zeta = c/c_\infty$; c_∞ = bulk concentration) reads

$$\zeta_{1,2} = \left(\frac{1 + \vartheta_{1,2} \exp -x/\lambda}{1 - \vartheta_{1,2} \exp -x/\lambda}\right)^2 = \zeta_{2,1}^{-1} \tag{1}$$

In the second case, the Schottky–Mott case,[11] we assume that one bulk majority carrier is depleted while the other (usually the dopant) is immobile. In this case the lack of mobile carriers results in a Gaussian profile ($x < \lambda^*$)

$$\zeta_2 = \exp -\left(\frac{x - \lambda^*}{2\lambda}\right)^2 \tag{2}$$

λ^* being the effective width in this case, is related to the Debye-length by the bulk defect chemistry of the phase under consideration via

$$\lambda^*/\lambda = \sqrt{8 \ln \frac{1 - \vartheta_2}{1 + \vartheta_2}} \tag{3}$$

The decisive parameter in eqns (1) and (2) is the ϑ parameter

$$\vartheta_{1,2} = \frac{\zeta_{1,2}^{1/2}(x = 0) - 1}{\zeta_{1,2}^{1/2}(x = 0) + 1} = -\vartheta_{2,1} \tag{4}$$

which measures the degree of influence[3] and thus the space charge effects due to the presence of the second phase. The connection of c_o with the core-chemistry and the decisive parameters can be a complicated conceptional problem and generally lacks experimental support. For a more detailed consideration see Refs 3, 4, and 9.

2.2 Charge transport across and along an interface

Even if the core structure can be viewed as being homogeneous, the complete interface is distinctly structured. It is at least a composite of core and space charge laver, the latter exhibiting a significant profile structure itself. So it matters very much whether the transport across or along an interface is considered.

The space charge contribution has to integrate over the local conductivity (parallel) or resistivity (serial). In the case of a carrier accumulation, we are interested in the excess conductivity parallel to the interface which reads in terms of λ and $\vartheta^{2,9}$ (L is the spatial extension covered by the electrode)

$$\Delta\sigma^{\|} = \frac{(2\lambda)Fu_1 2c_{1\infty}}{L}\,\frac{\vartheta_1}{1-\vartheta_1} \tag{5}$$

If a depletion layer occurs, we obtain for the excess resistivity,[2,9]

$$\Delta\rho^{\perp} = \begin{cases} \dfrac{2\lambda}{L}\dfrac{2}{Fu_1c_{1\infty}}\dfrac{|\vartheta_1|}{1+\vartheta_1} & \text{Gouy–Chapman} \\[2ex] \dfrac{\lambda(1-\vartheta_2)^2/(1+\vartheta_2)^2}{LFu_2c_{2\infty}\sqrt{2\ln\frac{1-\vartheta_2}{1+\vartheta_2}}} & \text{Schottky–Mott} \end{cases} \tag{6}$$

By taking into account capacitive effects we can define excess impedances or admittances, in both directions.

Special attention has to be paid to electrode interfaces, in particular if they are selectively reversible/blocking for different carrier types. Consider e.g. a mixed conducting electroceramic sandwiched between electrodes, which let through electrons but not ions (i.e. the respective reaction is kinetically hindered or even thermodynamically impossible). Then the sample becomes chemically polarised. We expect a space charge polarisation and a stoichiometric bulk polarisation.[6] The latter is called a Wagner–Hebb polarisation[12,13] and is usually used to determine transport coefficients. The effect may of course also be undesired and lead to serious long-time effects as analysed for ceramic capacitors in Ref. 14 The intermingling of space charge and bulk effects can become very tricky and has been qualitatively revisited recently.[5] The stoichiometric effects will be taken up again below.

Figure 1 gives an example of accumulation layers in composite solid electrolytes. AgU (also AgBr) has been 'heterogeneously doped' by $A1_2O_3$. Very fine alumina particles are sitting in the grain boundaries, setting appropriate boundary conditions for pronounced space charge effects.[3] Chemically speaking Ag^+ ions are adsorbed by the basic oxide's surface. As a consequence the boundary layers are (depleted of Ag^+ but) enriched in mobile vacancies. Since silver ion interstitials, the normal majority bulk carriers, are depleted we face, strictly speaking, an inversion layer. Similar effects are observed and have been analysed in composites consisting of two ionic conductors, as well as at surfaces and at grain boundaries of ionic conductors.[9] Surfaces and grain boundaries can be chemically conditioned by contamination with acidic or basic molecules (e.g. NH_3 for silver halides, BF_3 for alkaline earth fluorides etc). The same effect can be used as the analogue to a Taguchi-sensor for sensing acid-base-active gases.[15]

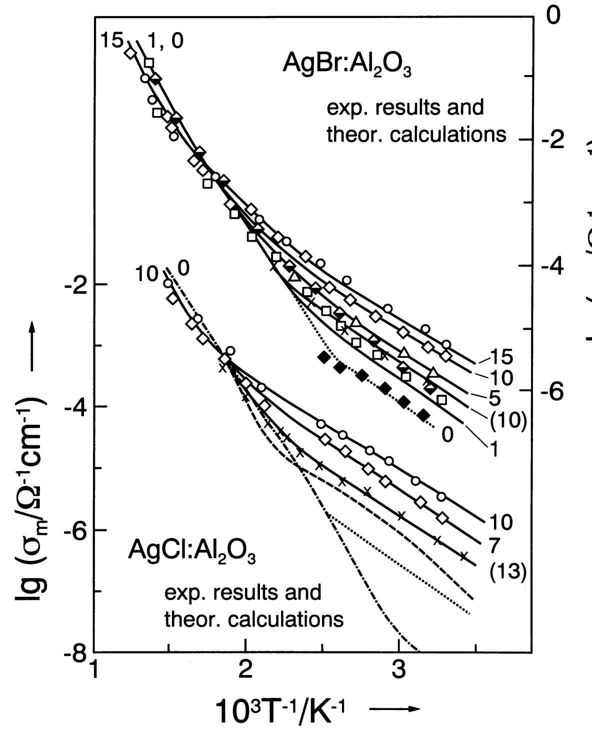

Fig. 1. Ionic space charge effects induced by the second phase ('Heterogeneous Doping') lead to a pronounced enhancement of the ionic conductivity.[3,9]

Figure 2 gives an example of a depletion-resistance in $SrTiO_3$.[16] There the electronic grain boundary resistance, a consequence of hole depletion, has been measured (see also Ref. 17). The P_{O_2}-dependence has been explained in Ref. 16. In polycrystalline $SrTiO_3$, different types of boundaries (different crystallography. differing structure and chemistry) have to be distinguished (some containing glass films).

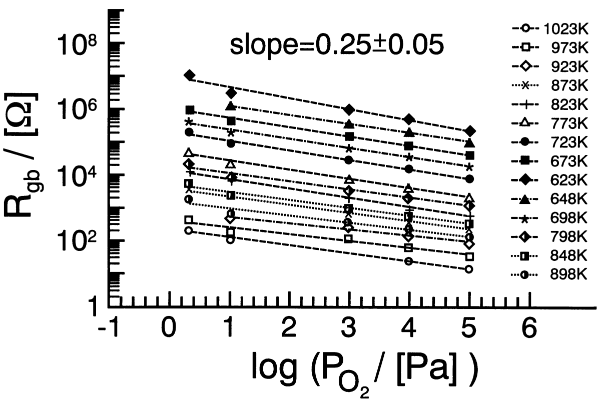

Fig. 2. Depletion resistance at a $SrTiO_3$ bicrystal boundary as a function of P_{O_2}.[16]

The above examples highlighted the significance of appropriate models for the superposition of bulk and boundary effects. Even though this can be done in a powerful way using finite element calculations, simple and analytically tractable models are useful.

In the following, we outline the brick-layer model generalised to parallel and serial core plus space charge effects as treated in Ref. 2.

2.3 Overall chemical properties: generalised brick-layer model

The bricklayer model uses a microstructure of primitive translational symmetry usually with cubic grains. The total unit cell includes two half grain boundaries in series and four half grain boundaries parallel to the current direction. Each grain boundary consists of core and space charge regions. (The effective contributions of the latter have been given by the above equations.) The total treatment is described in detail in Ref. 2. One point we immediately realise: owing to the anisotropy of the space charge profile and, in addition, due to the anisotropy of the space charge layer core sandwich, we definitely have to take account of different pathways in the same sample under the same conditions: bulk transport through and transport along the grain boundaries.

Let us consider the special case of an accumulation layer adjacent to a highly resistive core. Then in the direction parallel to the interface the space charge contribution will dominate. In the perpendicular direction, the core effect is decisive. The general complex overall conductivity reads ($\beta_L^{\|}$, $\beta_L^{\perp}$ measure the number of boundaries parallel and serial to the current direction, φ_L is the volume fraction of the boundaries):[2]

$$\widehat{\sigma}_m = \frac{\widehat{\sigma}_\infty\,\widehat{\sigma}_L^{\perp} + \beta_L^{\|}\varphi_L\,\widehat{\sigma}_L^{\|}\,\widehat{\sigma}_L^{\perp}}{\widehat{\sigma}_L + \beta_L^{\perp}\varphi_L\,\widehat{\sigma}_\infty} \tag{7}$$

Equation (7) is, in the limit $\omega \to 0$, also valid for σ instead of $\widehat{\sigma}$. Equation (7) immediately allows the analysis of the impedance spectrum. If the relaxation times are sufficiently different we will observe two semicircles. The high frequency semicircle is characterised by a bulk capacitance parallel to the bulk resistance which itself is parallel to (space charge) boundary resistances. The series boundary impedance (resistance parallel to the boundary capacitance) appears as a second semicircle. Thus, interfacial processes may appear in distinct frequency regimes. If annealing of such a ceramic leads to lowering of the grain boundary effects (e.g. through grain coarsening), obviously the low frequency semicircle will diminish (blocking effect decreases, limit: zero), while the left one will increase (short-circuiting pathways become less important, limit: pure bulk value). This has been observed for AgCl (see Fig. 3).[2] One point is worth mentioning: we assumed that at the intersection of parallel and serial boundaries the blocking effect dominates (as natural for our mechanism assumed), but there may be cases in which this is questionable. If the highly conducting effect dominates, the parallel pathways will short-circuit the total sample and the impedance spectrum is different.

The brick-layer model may also be used for composite electrolytes if the grain size and content of the second phase are small as realised for many halide alumina composites.[9] Even though the overall resistance (also the d. c. value) is decreased by orders of magnitude, the low frequency resistance contribution itself is increased. This is due to current constriction effects. The ionic current must force itself through the space left between the insulator particles. Such phenomena caused by lateral inhomogeneities are of pronounced significance in many cases of practical interest (e.g. for porous fuel cell electrodes).[7]

3 Interfacial Effects on Compositional Changes

The kinetics of compositional changes can generally be decomposed into (ambipolar) diffusion processes and interfacial processes (grain boundaries, surfaces).

The first can be described by a chemical diffusion coefficient D^δ and is comparably well understood.[18,19] Generally, it is composed of a chemical resistance term, R^δ_∞ (determined by the conductivities of the individual carriers) and a chemical capacitance, C^δ_∞, (inverse thermodynamic factor, determined by the defect concentrations). Equally, the interfacial processes may be described by effective rate constants ($\bar{k}^\delta$) which generally refer to a network of individual reaction steps. This is especially complex at surfaces where the proper chemical reaction takes place, e.g. the adsorption, dissociation, ionisation of oxygen, transfer of O^{2-} into the solid oxide including transport of both O^{2-} and e^- through the space charge region. But also at grain boundaries, we have at least two series steps (space-charge region, core) to be taken into consideration.

If we replace the interface by a 'black box' and if we assign the space co-ordinate 0 to the boundary between bulk and 'black box', we may define $\bar{k}^\delta$ by $-j/\delta c(\mathrm{O})$, δc being the deviation of the concentration from the equilibrium value.[20] It has been shown recently how $\bar{k}^\delta$ can be evaluated if the chemical storage capacity of the interface is negligible and one elementary rate step (rds) is determining.[21] The decisive resistive quantity then is the exchange rate of the rds. From this, the dependence of $\bar{k}^\delta$ on control parameters, the relationship with other effective rate

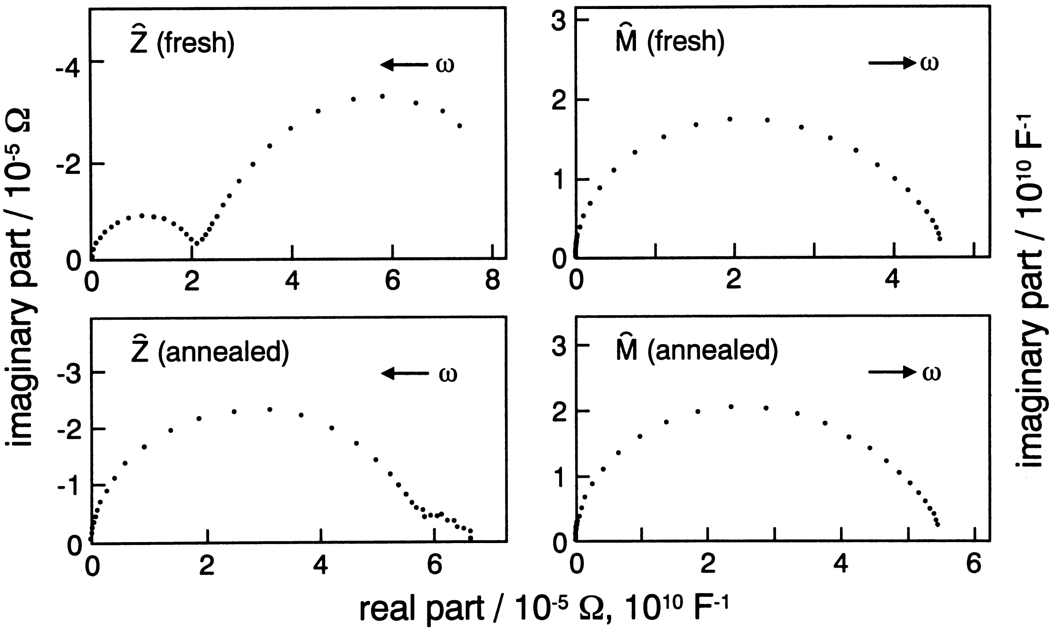

Fig. 3. Upon annealing the high frequency resistance increases (see impedance plots, l.h.s.) with the capacitance remaining constant (see modulus plots, r.h.s.). The low frequency resistance decreases. The interpretation is that upon annealing the influence of both highly conducting pathways and of blocking boundaries diminishes.[2]

constants determined from purely electrical experiments ($\bar{k}^Q$) or tracer experiments ($\bar{k}^*$), as well as with diffusion coefficients may be derived.[21]

Let us consider as an example the case that the rds for oxygen incorporation in an oxide with high electronic carrier concentration is the dissociative Langmuir adsorption of O_2 (with the rate constants $\overrightarrow{k}_s$ and $\overleftarrow{k}_s$), then[21]

$$\bar{k}^\delta/\Delta x = \sqrt{\overrightarrow{k}_s\overleftarrow{k}_s P_{O_2}^{1/2}[V_{ad}][O_{ad}]/[V_o^{\cdot\cdot}]^2} \qquad (8)$$

$[V_o^{\cdot\cdot}]$ is the vacancy concentration at $x=0$ and Δx the distance from there to the adsorption layer. $[V_O^{\cdot\cdot}]$ as well as the surface concentrations $[V_{ad}]$, $[O_{ad}]$ can be expressed in terms of mass action constants. Given that the same rds determines tracer exchange, $\bar{k}^*$ is $\bar{k}^\delta$ times mole fraction of the vacancies (at $x=0$).

Figure 4 displays space resolved in-situ profiles for the diffusion-limited and surfacelimited oxygen incorporation in $SrTiO_3$ from which $\bar{k}^\delta$ and D^δ can be elegantly determined.[22]

In space charge regions, a chemical diffusion coefficient is no longer an appropriate transport coefficient if the transient case is considered. Ionic and electronic fluxes are then no longer coupled in a simple way.[20] The accurate calculation is quite complex and three qualitative remarks may suffice: (i) jam effects may occur at the boundary; (ii) the dependence of the transport rate on the space charge potential (i.e. ϑ) can be surprising, and (iii) space charges are built-up in the transient even if there have been no initial space charge layers. Details are described in Ref. 20.

As far as chemical transport in polycrystalline materials is concerned, we have again a superposition of parallel and serial effects. Again it may be described using a bricklayer model and again flux constriction may be important. While the serial boundaries will be most 'visible' if they act blocking, the parallel ones may effectively serve as short-circuiting mass transport pathways. The latter phenomenon is especially complex since the rapid stoichiometric changes occurring via boundaries create also driving force components in the perpendicular direction.

Two simple formulae can be given for the following extreme cases in the framework of the brick-layer model. The mass transport along boundaries is much faster than via the bulk. Then the effective diffusion length will be the grain size (L_g) rather than the sample size (L)

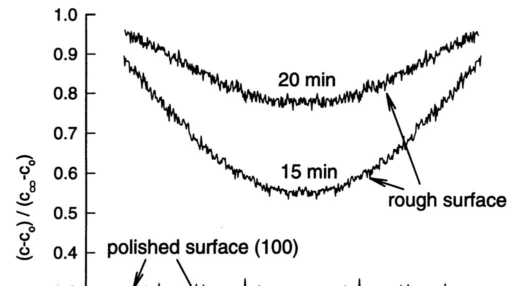

Fig. 4. In-situ concentration profiles as a function of space and time. The upper two curves indicate diffusion control while the lower one indicates surface rate control. The switch-over can e.g. be induced by roughening/polishing.[22]

$$D^{\delta}_{m} \propto \frac{L^2 \sigma^{\delta}_{\infty}}{L^2_g c^{\delta}_{\infty}} \tag{9}$$

(As mentioned above we decompose D^{δ} into a chemical resistance $R^{\delta}_{\infty} \propto (\sigma^{\delta}_{\infty})^{-1}$ and a chemical capacitance $C^{\delta}_{\infty} \propto (c^{\delta}_{\infty})^{-1}$. It holds that: $(\sigma^{\delta}_{\infty})^{-1} \propto \sigma^{-1}_{\mathrm{eon}} + \sigma^{-1}_{\mathrm{ion}}$; $(c^{\delta}_{\infty})^{-1} \propto c^{-1}_{\mathrm{ion}} + 4c^{-1}_{\mathrm{eon}}$ if no trapping occurs). This is a well-known result.

Recently a similarly simple result was shown to be valid[23] if the polycrystalline material is dominated by boundaries blocking to chemical transport. It is assumed that the boundaries are thin enough that the chemical storage in these can be neglected compared to the bulk.

$$D^{\delta}_{m} \propto \frac{L_g \sigma^{\delta}_{gb}}{L_{gb} c^{\delta}_{\infty}} \tag{10}$$

Now R^{δ} and σ^{δ} derive from a series switching of ionic and electronic conductivities in the boundary while C^{δ} and c^{δ}_{∞} still refer to the bulk.

4 Nano-size Effects on Electrical and Chemical Transport

Nano-size effects (see e.g. Ref. 24) can be decomposed into two parts. The first and more conventional one, is solely determined by scaling down the interface–volume ratio of the macroscopic samples, the specific quantities being invariant. The second one includes mesoscopic phenomena, i.e. size dependencies of specific quantities. The first point refers e.g. to the increased free energy and also changed conductances due to a larger surface-to-volume ratio. It also refers to a higher density of edges and corners if the size is reduced. Already such phenomena are sufficient to change e.g. the melting point of metals by several hundreds of K,[25] or to vary the overall conductivity of a polycrystalline material significantly. In nano-crystalline CaF_2 the conductivity is enhanced by several orders of magnitude.[26]

More striking are phenomena of the second class. In our context, they are obviously met for space charge effects if the grain size or more generally the distance between the interfaces drops below 4 times the Debye length (or $2\lambda^*$ for Schottky–Mott depletion layers). This mesoscopic effect has been predicted and quantitatively discussed in Ref. 27. Its relevance for nano-crystalline electroceramics is obvious. A very recent application was the interpretation of the conductivities in the AgI–Al_2O_3 nano-composite.[28] There, a so-called 7H phase (as shown in Fig. 5) forms at the Al_2O_3/AgI interface which can be conceived as a β– and γ-heterostructure alternating with a structural wave length below the Debye-length.

The additional conductivity increase in the accumulation case is described by the[27]

$$\text{nano-sizefactor} = \frac{4\lambda}{L_g}\left[(c_o - c(\text{grain center}))/c_o\right]^{1/2} \tag{11}$$

The concentration in the grain center is a complicated but defined function of c_o and L_g. The last experimental example involved structural variations which certainly come into play if we approach the regime of cluster chemistry.[29] Then a second mesoscopic length scale comes into play.[30] Thermodynamically speaking the chemical standard potential becomes a function of size. Such a size dependence is rather common for electronic conductors in quantum devices. There it is mostly due to the fact that the electron wave function is effectively extended, perceives both boundaries and the energy levels become sensitive functions of the distance ($\propto L^2_g$). In the case of the ionic defects, structural effects are necessary to change μ^{o}.

5 Phase Transitions at Interfaces

The AgI–Al_2O_3 composite (see Fig. 5) is not only an example of such mesoscopic effects, it also

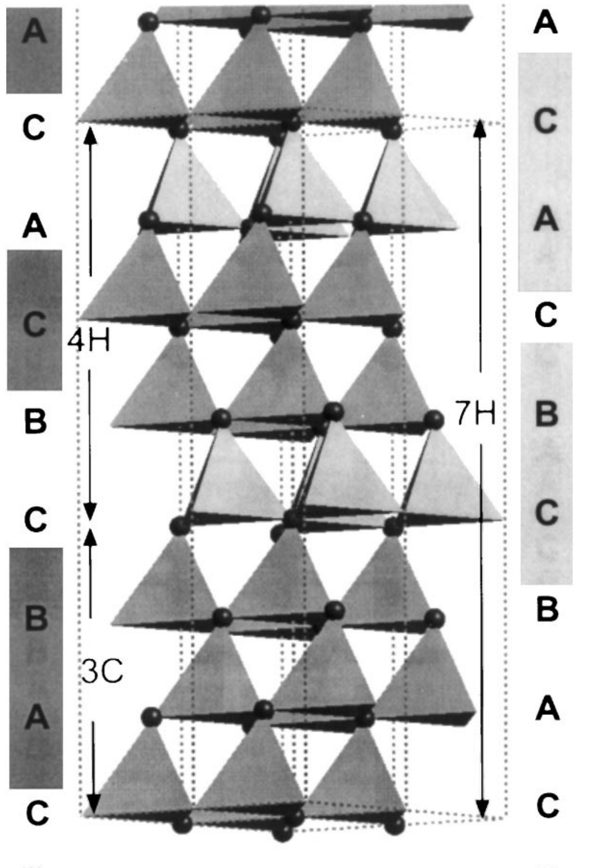

Fig. 5. Stacking fault phase forming at the β-AgI–Al_2O_3 contacts. It can be conceived as a nano-sized heterostructure with a pronounced disorder in the cation sublattice.

highlights the relevance of phase transitions at interfaces. Their appearance in equilibrium is of course a question of interfacial thermodynamics.[31] Nevertheless, it is interesting to note that some transitions of this kind may be mechanistically understood as a necessary consequence of charge carrier interaction.[1,30] On one hand, it can be shown that carrier interaction necessarily 'lead' to phase transformations in the bulk.[32,33] On the other hand, carrier interactions are different at boundaries. Thus, it is reasonable to expect phase transformations at interfaces to occur at temperatures different from the bulk transition.

The manifold of properties occurring at interfaces do not only complicate the understanding of electroceramics but also allow for a variety of optimisation strategies.

Acknowledgements

The author is indebted to Harry L. Tuller for discussions and reading the manuscript.

References

1. Maier, J., *Proc. Int. School on Oxygen Ion and Mixed Cond.*, I. Riess, H. L. Tuller, J. Schoonman, Kluwer, Dordrecht, The Netherlands, in press.
2. Maier, J., On the conductivity of polycrystalline materials. *Ber. Bunsenges. Phys. Chem.*, 1986, **90**, 26–33.
3. Maier, J., Defect chemistry and conductivity effects in heterogenous solid electrolytes. *J. Electrochem. Soc.*, 1987, **134**, 1524–1535.
4. Jamnik, J., Maier, J. and Pejovnik, S., Interfaces in solid ionic conductors: Equilibrium and small signal picture. *Solid State Ionics*, 1995, **75**, 51–58.
5. Jamnik, J. and Maier, J., Why do not all conductors exhibit Warburg diffusion under selectively blocking conditions? *J. Electrochem. Soc. Letters*, submitted for publication.
6. Maier, J., Electrochemical investigation methods of ionic transport properties in solids. *Solid State Phenomena*, 1994, **39–40**, 35–60.
7. Fleig, J. and Maier, J., The influence of current constriction on the impedance of polarisable electrodes: Application to the fuel cell electrodes. *J. Electrochem. Soc. Letters*, 1997, **144**, L302–L305.
8. Wolf, D. in *Materials Interfaces. Atomistic-level Structure and Properties*, ed D. Wolf and S. Yip. Chapman and Hall, London, 1992, pp. 1–58.
9. Maier, J., Ionic conduction in space charge regions. *Prog. Solid St. Chem.*, 1995, **23**, 171–263.
10. Kliewer, K. L. and Köhler, J. S., Space charge in ionic crystals. I. General approach with application to NaCl. *Phys. Rev.*, 1995, **140**, A1226–A1240.
11. Sze, S. M., *Physics of Semiconductor Devices*. Wiley-Interscience, New York, 1981.
12. Wagner, C., Galvanic cells with solid electrolytes involving ionic and electronic conduction in *Proc. 7th Meeting Int. Comm. on Electrochem. Thermodynamics and Kinetics*, Lindau, 1955. Butterworth, London, 1957, pp. 361–375.
13. Yokota, I., On the theory of mixed conduction with special reference to the conduction in silver sulfide group semiconductors. *J. Phys. Soc. Japan*, 1961, **16**, 2213–2223.
14. Waser, R., Baiatu, T. and Härdtl, K.-H., dc electrical degradation of perovskite-type titanates: *J. Am. Ceram. Soc.*, 1990, **73**, 1645–1653.
15. Maier, J., Heterogenous solid electrolytes, in *Recent Trends in Superionic Solids and Solid Electrolytes,* ed. S. Chandra, A. Laskar. Academic Press, New York, 1989, pp. 137–184; Maier, J., Electrical sensing of complex gaseous species by making use of acid-base properties. *Solid State Ionics*, 1993, **62**, 105–111.
16. Denk, I., Claus, J. and Maier, J., Electrochemical investigations of $SrTiO_3$ boundaries. *J. Electrochem. Soc.* 1997, **144**, 3526–3536.
17. Vollmann, M. and Waser, R., Grain boundary defect chemistry of acceptor-doped titanites: Space charge layer width. *J. Am. Ceram. Soc.*, 1994, **77**, 235–243.
18. Heyne, L., Electrochemistry of mixed ionic-electronic conductors, in *Solid Electrolytes*, ed. S. Geller. Springer-Verlag, Berlin, 1977, pp. 169–221.
19. Maier, J., Mass transport in the presence of internal defect reactions—Concept of Conservative Ensembles. Part I: Chemical diffusion in pure compounds. *J. Am. Ceram. Soc.*, 1993, **76**(5), 1212–1217.
20. Jamnik, J. and Maier, J., Transport across boundary layers in ionic crystals. Part I: General formalism and conception. *Ber. Bunsenges. Phys. Chem.*, 1997, **101**, 23–40.
21. Maier, J., Point defect thermodynamics and size effects. *Solid State Ionics*, in press.
22. Leonhardt, M., Claus, J. and Maier, J., in preparation.
23. Jamnik, J. and Maier, J., Chemcal diffusion through grain boundaries in mixed conductors. *J. Electrochem. Soc.*, 1998, **145**, 1762–1767.
24. Chiang, Y.-M. (ed.), Special issue on nanostructured materials for energy applications. *J. Electroceramics*, 1997, **3**.
25. Buffat, Ph. and Borel, J.-P., Size effect on the melting temperature of gold particles. *Phys. Rev. A*, 1976, **13**, 2287–2298.
26. Puin, W., Rodewald, S., Heitjans, R., Ramlau, R. and Maier, J., Local and overall ionic conductivity in nanocrystalline CaF_2, *Solid State Ionics*, in press.
27. Maier, J., Space charge regions in two solid phase systems and their conduction contribution–III: Defect chemistry and ionic conductivity in thin films. *Solid State Ionics*, 1987, **23**, 59–67; Maier, J., Prill, S. and Reichert, B., Space charge effects in plycrystalline, micropolycrystalline and thin film samples: Application to AgCl and AgBr. *Solid State Ionics*, 1988, **28–30**, 1465–1469.
28. Lee, J.-S., Adams, St. and Maier, J., Defect chemistry and transport characteristics β-AgI, in preparation.
29. Martin, T. P., The structure of elemental; and molecular clusters in: *Festkörperprobleme (Advances in Solid State Physics)* ed. P. Grosse. Vieweg, Braunschweig, 1984, **XXIV**, pp. 1–24.
30. Maier, J., *Solid State Ionics*, in preparation.
31. Lipowsky, R., *Phasenübergänge Oberflächen* (IFF Ferienkurs), FZ Jülich GmbH, Germany, 1993, pp. 9.1; *Springer Tracts in Mod. Phys.*, Vol. 127.
32. Huberman, R. A., Cooperative phenomena in solid electrolyts. *Phys. Rev. Lett.*, 1974, **32**, 1000–1002.
33. Hainovsky, N. and Maier, J., Simple phenomenological approach to premelting and sublattice melting in Frenkel disordered ionic crystals. *Phys. Rev. B*, 1995, **51**, 15789–15797.